

High-energy monitoring of Seyfert galaxies: the case of NGC 4593

F. Ursini^{1,2,3,*}, P.-O. Petrucci^{1,2}, G. Matt³, S. Bianchi³, M. Cappi⁴, B. De Marco⁵, A. De Rosa⁶, J. Malzac^{7,8}, and G. Ponti⁵

¹ Univ. Grenoble Alpes, IPAG, F-38000 Grenoble, France

² CNRS, IPAG, F-38000 Grenoble, France

³ Dipartimento di Matematica e Fisica, Università degli Studi Roma Tre, via della Vasca Navale 84, 00146 Roma, Italy

⁴ INAF-IASF Bologna, Via Gobetti 101, I-40129 Bologna, Italy

⁵ Max-Planck-Institut für extraterrestrische Physik, Giessenbachstrasse, D-85748 Garching, Germany

⁶ INAF/Istituto di Astrofisica e Planetologia Spaziali, via Fosso del Cavaliere, 00133 Roma, Italy

⁷ Université de Toulouse, UPS-OMP, IRAP, Toulouse, France

⁸ CNRS, IRAP, 9 Av. colonel Roche, BP44346, F-31028 Toulouse cedex 4, France

The dates of receipt and acceptance should be inserted later

Key words galaxies: active – galaxies: Seyfert – X-rays: galaxies – X-rays: individuals (NGC 4593)

We discuss preliminary results from a joint *XMM-Newton* and *NuSTAR* monitoring program on the active galactic nucleus NGC 4593, consisting of 5×20 ks observations, spaced by two days, performed in January 2015. The source is found to be variable, both in flux and spectral shape, on time scales as short as a few ks. The spectrum clearly softens when the source brightens. A simple timing analysis suggests the presence of a variable soft excess that correlates with the primary continuum.

© WILEY-VCH Verlag GmbH & Co. KGaA, Weinheim

1 Introduction

The central engine of active galactic nuclei (AGNs) is thought to be powered by accretion of surrounding matter onto a supermassive black hole. According to the standard paradigm, the accretion disc is responsible for the optical/UV emission, while the most likely origin of the X-ray emission is thermal Comptonization of the soft photons emitted by the disc in a hot region, the so-called corona (see, e.g., Haardt & Maraschi 1991; Haardt et al. 1994, 1997). This process is naturally able to explain the power-law shape of the observed X-ray spectrum of AGNs. A signature of thermal Comptonization is the presence of a high-energy cut-off, which is found in a number of cases (see, e.g., Ballantyne et al. 2014; Baloković et al. 2015; Brenneman et al. 2014; Malizia et al. 2014; Marinucci et al. 2014; Perola et al. 2002; Ursini et al. 2015). The primary X-ray emission can be modified by diverse processes, such as absorption from neutral or ionized gas, and Compton reflection from the disc or more distant material, like the putative obscuring torus. Moreover, a smooth rise below 1–2 keV above the extrapolated high-energy power law is commonly observed in the spectra of AGNs (see, e.g., Bianchi et al. 2009). The origin of this so-called soft excess is still uncertain (see, e.g., Done et al. 2012). Ionized reflection provides a good explanation in a number of sources (see, e.g., Walton et al. 2013), while a warm Comptonization mechanism is favoured in other cases (see, e.g., Boissay et al. 2014).

The current understanding of the geometrical and physical properties of the X-ray corona is far from being complete. Multiple, broad-band observations with a high signal-to-noise ratio are needed to disentangle the different spectral components through the analysis of their variability and constrain their characteristic parameters. This approach has proven successful to study the origin of the high-energy emission in Seyfert galaxies, as shown by recent campaigns on Mrk 509 (Kaastra et al. 2011; Petrucci et al. 2013) and NGC 5548 (Kaastra et al. 2014; Ursini et al. 2015). In particular *NuSTAR*, thanks to its dramatically improved signal-to-noise up to ~ 80 keV, allows for the study of the high-energy emission of AGNs with high precision (see, e.g., the review by Marinucci et al., presented in these proceedings).

NGC 5548 was the object of a long, multiwavelength campaign conducted from May 2013 to February 2014, with the main goal of studying its persistent ionized outflow, the so-called warm absorber (Kaastra et al. 2014). During the campaign, the nucleus was surprisingly found to be obscured by a fast, massive and clumpy stream of gas never seen before in this source. The properties of this obscuring outflow are consistent with those of a disc wind (Kaastra et al. 2014). The detailed description of the campaign is given by Mehdipour et al. (2015), while the physical and temporal properties of the outflows are described in Arav et al. (2015) and Di Gesu et al. (2015). Using the high-energy *XMM-Newton*, *NuSTAR* and

* Corresponding author: e-mail: francesco.ursini@obs.ujf-grenoble.fr

INTEGRAL data from the campaign, Ursini et al. (2015) studied the broad-band (0.3–400 keV) X-ray spectrum of NGC 5548. A high-energy cut-off of 70^{+40}_{-10} keV, attributed to thermal Comptonization, is found in one observation out of seven, while a lower limit ranging from 50 to 250 keV is found in the other six observations. The reflection component is consistent with being constant, thus it is likely produced by material lying a few light months away from the primary source. Furthermore, the average spectrum is well fitted by a Comptonized component produced by a corona with a temperature $kT_e = 40^{+40}_{-10}$ keV and an optical depth $\tau = 2.7^{+0.7}_{-1.2}$, assuming a spherical geometry.

The long-term campaign on NGC 5548 provided a detailed “anatomy” of that AGN. However, multiple observations on shorter time scales are equally important to make progress in the physical interpretation of the high-energy emission of AGNs. In the following, we discuss preliminary results from a monitoring program on the AGN NGC 4593 with *XMM-Newton* and *NuSTAR*. We focus on a phenomenological timing analysis, while the spectral analysis will be presented in a forthcoming paper. In Sec. 2 we describe the observations and an analysis of the temporal properties of the source. In Sec. 3, we summarize our results and conclusions.

2 The high-energy view of NGC 4593

NGC 4593 ($z = 0.009$, Strauss et al. 1992) is an X-ray bright Seyfert 1 galaxy, hosting a supermassive black hole of $(9.8 \pm 2.1) \times 10^6$ solar masses (Denney et al. 2006). Previous observations of this source with *BeppoSAX* (Guainazzi et al. 1999), *XMM-Newton* (Brenneman et al. 2007; Reynolds et al. 2004) and *Suzaku* (Markowitz & Reeves 2009) have shown a strong reflection hump above 10 keV (Guainazzi et al. 1999; Markowitz & Reeves 2009) and the presence of two narrow emission features due to neutral and hydrogen-like Fe K α lines at 6.4 and 6.97 keV respectively (Brenneman et al. 2007; Markowitz & Reeves 2009; Reynolds et al. 2004). Reynolds et al. (2004) found the full width at half-maximum (FWHM) of the neutral Fe K α line to be ~ 11000 km s $^{-1}$ using a 2002 *XMM-Newton* observation, significantly larger than the FWHM of the H β line, i.e. 4900 ± 300 km s $^{-1}$ (Grupe et al. 2004). This result seems to suggest that the Fe K α line-emitting material lies significantly inside the broad-line region (BLR). However, Markowitz & Reeves (2009) found the FWHM of the Fe K α line to be ~ 4000 km s $^{-1}$ in a 2007 *Suzaku* observation, suggesting emission from at least 5000 gravitational radii. The Fe K α line-emitting region seems therefore to be changing with time. A soft excess below 2 keV was found both in the 2002 *XMM-Newton* data (Brenneman et al. 2007) and in the 2007 *Suzaku* data, albeit with a drop in the 0.4–2 keV flux by a factor > 20 in the latter (Markowitz & Reeves 2009). Finally, Guainazzi et al. (1999) found only

Table 1 The logs of the joint *XMM-Newton* and *NuSTAR* observations of NGC 4593.

Obs.	Satellites	Obs. Id.	Start time (UTC) yyyy-mm-dd	Net exp. (ks)
1	<i>XMM-Newton</i> <i>NuSTAR</i>	0740920201 60001149002	2014-12-29	16 22
2	<i>XMM-Newton</i> <i>NuSTAR</i>	0740920301 60001149004	2014-12-31	17 22
3	<i>XMM-Newton</i> <i>NuSTAR</i>	0740920401 60001149006	2015-01-02	17 21
4	<i>XMM-Newton</i> <i>NuSTAR</i>	0740920501 60001149008	2015-01-04	15 23
5	<i>XMM-Newton</i> <i>NuSTAR</i>	0740920601 60001149010	2015-01-06	21 21

a lower limit on the high-energy cut-off of 150 keV using *BeppoSAX* data.

2.1 Observations and data reduction

XMM-Newton (Jansen et al. 2001) and *NuSTAR* (Harrison et al. 2013) performed five joint observations of NGC 4593, ~ 20 ks each, spaced by two days, starting from 2014 December 29. The log of the data sets is reported in Table 1.

In the *XMM-Newton* observations, the EPIC instruments were operating in the Small-Window mode with the thin-filter applied. For simplicity, we used the EPIC-pn data only for our analysis. The data were processed using the *XMM-Newton* Science Analysis System (SAS v13). Source extraction radii and screening for high-background intervals were performed through an iterative process which leads to a maximization of the signal-to-noise ratio, as described in Piconcelli et al. (2004).

The *NuSTAR* data were reduced with the standard pipeline (NUPIPELINE) in the *NuSTAR* Data Analysis Software (NUSTARDAS, v1.3.1; part of the HEASOFT distribution as of version 6.14), using calibration files from *NuSTAR* CALDB v20150316. Spectra and light curves were extracted from the cleaned event files using the standard tool NUPRODUCTS for each of the two hard X-ray detectors aboard *NuSTAR*, which sit inside the corresponding focal plane modules A and B (FPMA and FPMB). The source data were extracted from circular regions with a radius of 75 arcsec, and background was extracted from a blank area close to the source.

2.2 Timing analysis

The light curves of the five observations are shown in Fig. 1. Strong flux variability, particularly in the soft band, is found on time scales of a few ks. In Fig. 2, we show the *XMM-Newton*/pn (2–10 keV)/(0.5–2 keV) hardness ratio plotted against the *XMM-Newton*/pn count rate in the 0.5–10 keV band, and the *NuSTAR* (10–50 keV)/(3–10 keV) hardness ratio plotted against the *NuSTAR* count rate in the 3–50 keV band. These plots show that a higher flux corresponds to a

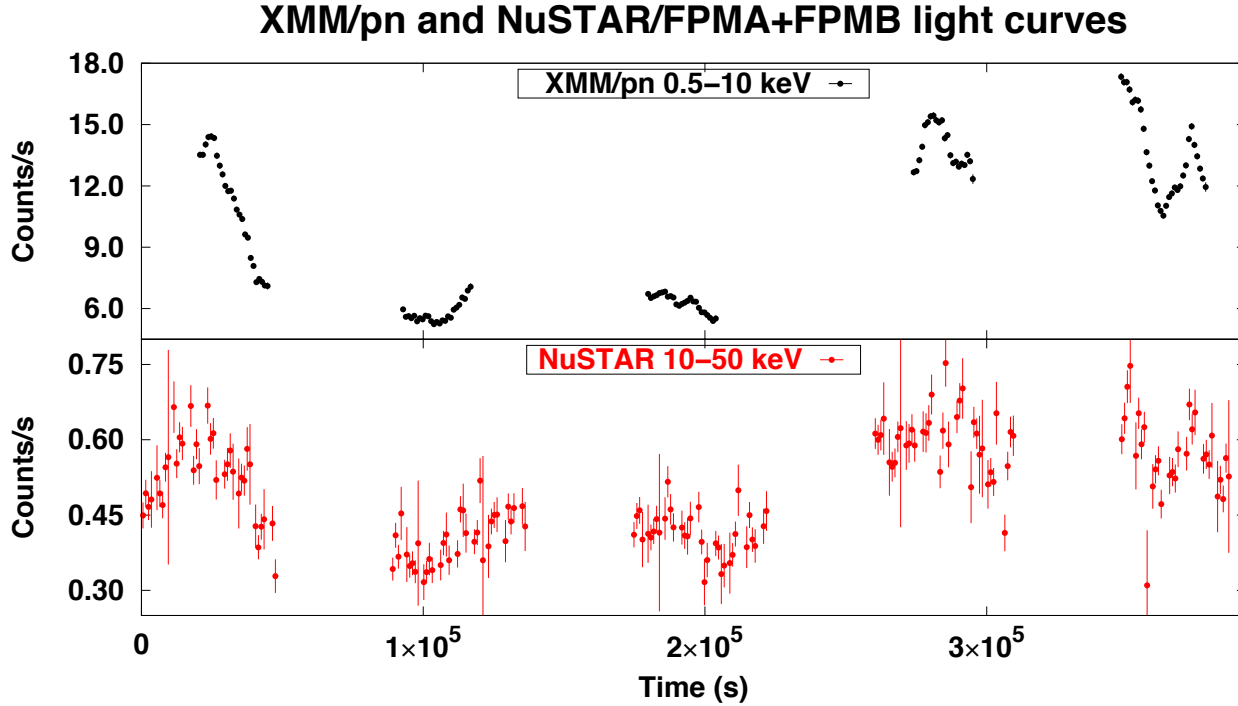


Fig. 1 Count-rate light curves of the five joint *XMM–Newton* and *NuSTAR* observations of NGC 4593. Bins of 1 ks are used. Top panel: *XMM–Newton*/pn light curves in the 0.5–10 keV band. Bottom panel: *NuSTAR* light curves (co-adding FPMA and FPMB data) in the 10–50 keV band.

lower hardness ratio, i.e. the typical “softer when brighter” behaviour. Furthermore, the spectral variability is especially prominent in the soft band. This is also apparent from the *XMM–Newton*/pn and *NuSTAR* spectra shown in Fig. 3. The detailed spectral analysis is beyond the scope of this article, and is deferred to a future work (Ursini et al., in prep.).

In Fig. 4 we plot the *XMM–Newton*/pn count rate in the 3–5 keV range against the *XMM–Newton*/pn count rate in the 0.3–0.5 keV range. The 0.3–0.5 keV band is likely dominated by the soft excess (Brenneman et al. 2007; Markowitz & Reeves 2009), while the 3–5 keV band is dominated by the primary power law-like emission with no significant contribution from the reflection component. The plot shows a clear linear relationship between the two energy bands.

3 Discussion and conclusions

We reported the first results from five joint *XMM–Newton* and *NuSTAR* observations of NGC 4593. The high-quality, broad-band data clearly show both flux and spectral variability on time scales as short as a few ks. The spectral variability is particularly prominent in the soft band, namely below 10 keV. Since the spectra do not show signatures of strong absorption, the observed variability appears to be intrinsic. The analysis of the hardness ratio provides a model-independent evidence that the spectrum

is softer when the flux is higher, which corresponds to the “softer when brighter” behaviour generally found in luminous Seyfert galaxies (see, e.g., Sobolewska & Papadakis 2009; Soldi et al. 2014). This behaviour can be understood as an effect of Comptonization, since an increase of the soft seed photon luminosity, due for example to a higher accretion rate, results in a more efficient cooling of the hot corona via inverse Compton scattering. A lower coronal temperature in turn determines the steepening of the spectrum.

The data show a linear relationship between the fluxes in the 3–5 keV energy band and in the 0.3–0.5 keV band, where the expected dominant components are the primary power law and the soft excess, respectively. This linear relationship suggests a common physical origin for the hard X-ray emission and the soft excess. If the hard X-ray emission is due to Comptonization, this result is consistent with the soft excess being produced via Comptonization of the same seed photons (see also Brenneman et al. 2007; Markowitz & Reeves 2009). This may in turn suggest the presence of both a “hot” corona with a temperature of 10–100 keV, which is responsible for the hard X-ray emission, and a “warm” corona with a lower temperature (e.g. ~ 0.5 keV), which is responsible for the soft excess (for a detailed discussion of this scenario, see Petrucci et al. 2013). In this case, geometrical or physical variations of the accretion disc/corona system, such as changes in the

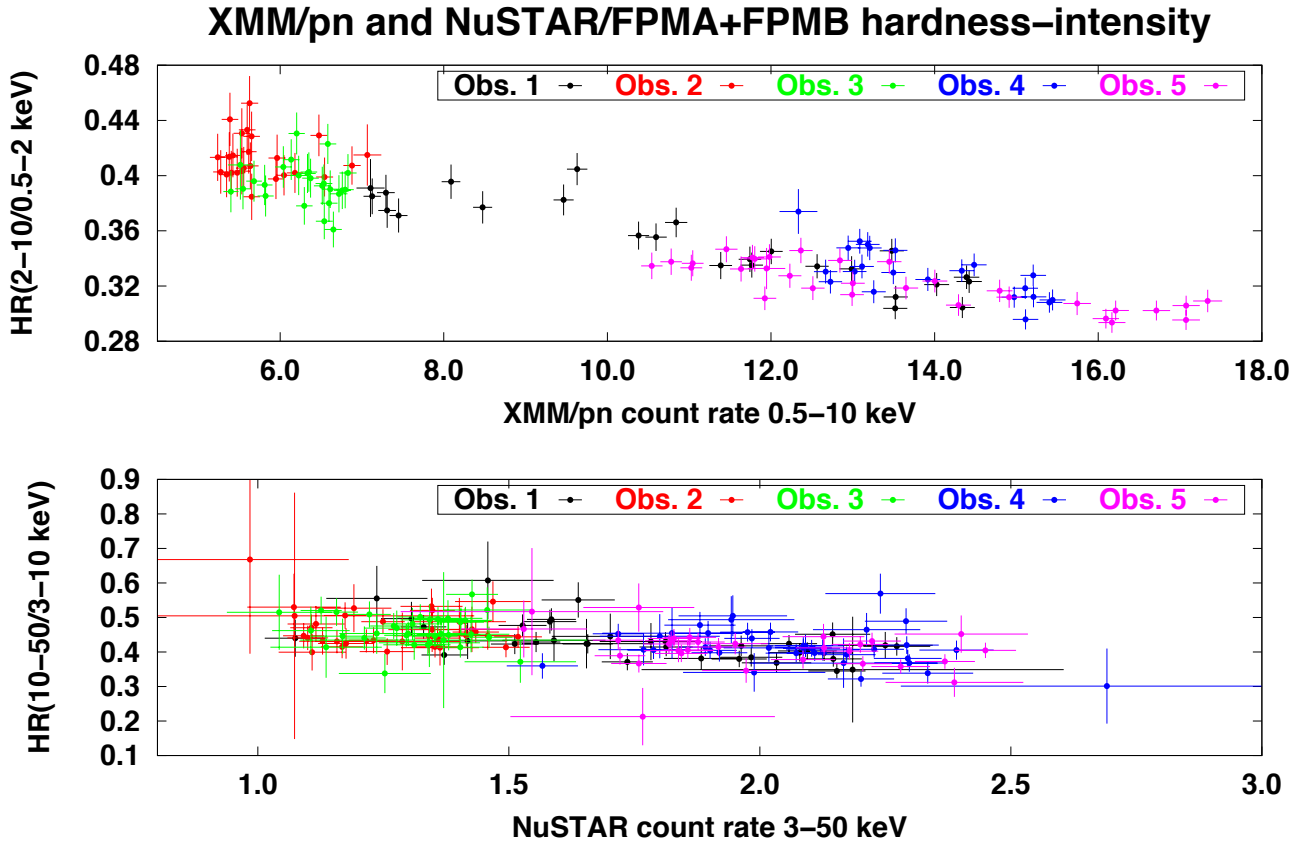


Fig. 2 “Hardness-intensity diagram” of the five joint *XMM-Newton* and *NuSTAR* observations of NGC 4593. Each point corresponds to a time bin of 1 ks. Top panel: *XMM-Newton*/pn hardness ratio (2–10 keV)/(0.5–2 keV) plotted against the 0.5–10 keV count rate. Bottom panel: *NuSTAR*/FPMA+FPMB hardness ratio (10–50 keV)/(3–10 keV) plotted against the 3–50 keV count rate.

accretion rate, could account for both the soft excess and primary continuum variability.

A detailed spectral analysis, with the study of the soft excess and the reflection component, will be presented in a forthcoming paper, also including the UV data from the *XMM-Newton* Optical Monitor, which may carry useful informations to study the Comptonization components (see, e.g., Petrucci et al. 2013). We stress that this is the first *XMM-Newton*+*NuSTAR* monitoring program explicitly aimed at the study of the high-energy emission of an AGN through its variability on time scales of days down to a few ks. In the framework of a previous campaign on NGC 5548, conducted over a few months, the broad-band coverage of *XMM-Newton*, *NuSTAR* and *INTEGRAL* allowed us to study the high-energy spectrum of that source in detail (Ursini et al. 2015). The approach based on multiple, broad-band observations appears to be very promising for a better understanding of the processes associated with the high-energy emission of AGNs. Besides, further studies on a greater number of sources will be needed to investigate the similarities and differences between different types of AGNs.

Acknowledgements

We are grateful to the referee, Erin Kara, for comments that improved the paper.

This work is based on observations obtained with: the *NuSTAR* mission, a project led by the California Institute of Technology, managed by the Jet Propulsion Laboratory and funded by NASA; *XMM-Newton*, an ESA science mission with instruments and contributions directly funded by ESA Member States and the USA (NASA). This research has made use of data, software and/or web tools obtained from NASA’s High Energy Astrophysics Science Archive Research Center (HEASARC), a service of Goddard Space Flight Center and the Smithsonian Astrophysical Observatory. FU, POP, GM, SB, MC, ADR and JM acknowledge support from the french-italian International Project of Scientific Collaboration: PICS-INAF project number 181542. FU, POP acknowledge support from CNES. FU acknowledges support from Université Franco-Italienne (Vinci PhD fellowship). FU, GM acknowledges financial support from the Italian Space Agency under grant ASI/INAF I/037/12/0-011/13. SB and MC acknowledges financial support from the Italian Space Agency under

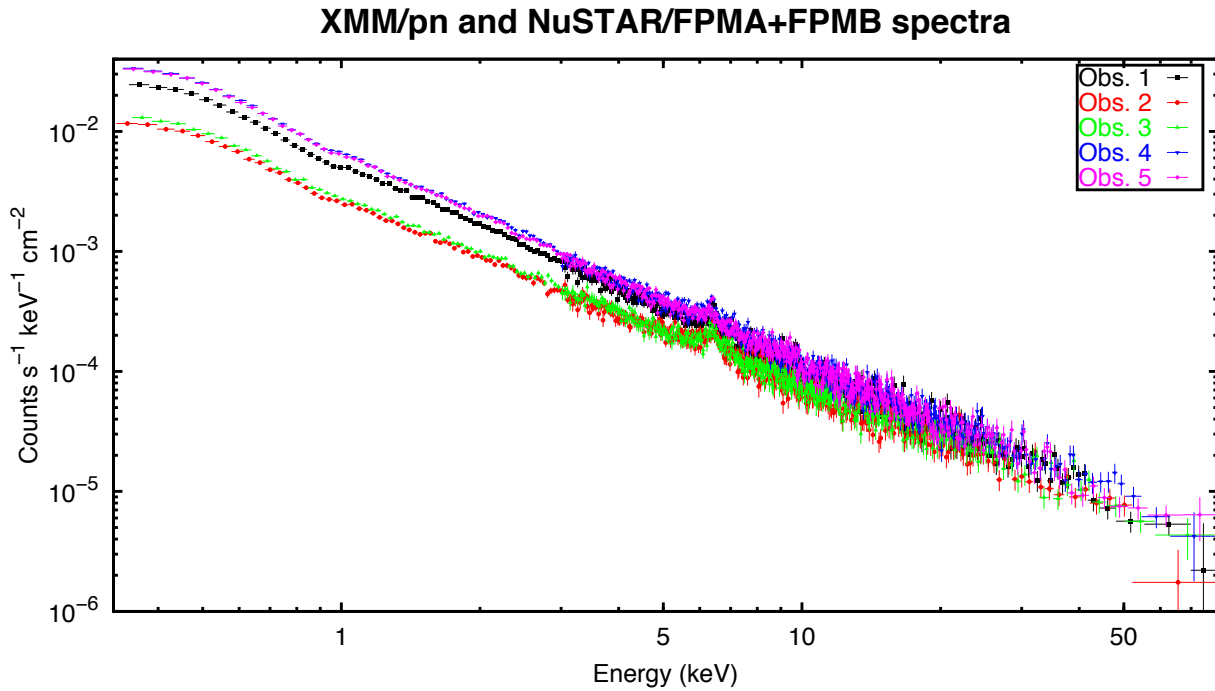


Fig. 3 The *XMM-Newton*/pn and *NuSTAR*/FPMA and FPMB data have been co-added for plotting purposes.

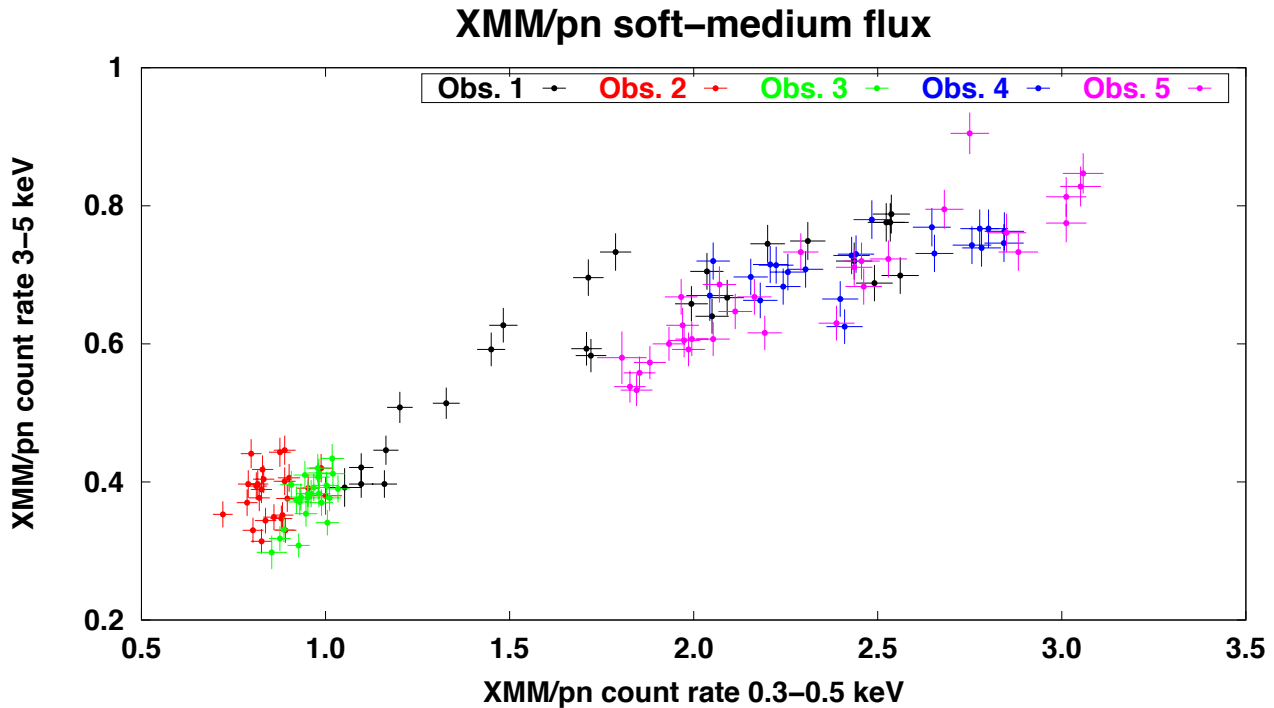


Fig. 4 *XMM-Newton*/pn count rate in the 3–5 keV range plotted against the *XMM-Newton*/pn count rate in the 0.3–0.5 keV range. Each point corresponds to a time bin of 1 ks.

grant ASI-INAF I/037/12/P1. GP acknowledges the Bundesministerium für Wirtschaft und Technologie/Deutsches Zentrum für Luft- und Raumfahrt (BMWi/DLR, FKZ 50 OR 1408) and the Max Planck Society for support.

References

- Arav, N., Chamberlain, C., Kriss, G. A., et al. 2015, *A&A*, 577, A37
- Ballantyne, D. R., Bollenbacher, J. M., Brenneman, L. W., et al. 2014, *ApJ*, 794, 62
- Baloković, M., Matt, G., Harrison, F. A., et al. 2015, *ApJ*, 800, 62
- Bianchi, S., Guainazzi, M., Matt, G., Fonseca Bonilla, N., & Ponti, G. 2009, *A&A*, 495, 421
- Boissay, R., Paltani, S., Ponti, G., et al. 2014, *A&A*, 567, A44
- Brenneman, L. W., Madejski, G., Fuerst, F., et al. 2014, *ApJ*, 788, 61
- Brenneman, L. W., Reynolds, C. S., Wilms, J., & Kaiser, M. E. 2007, *ApJ*, 666, 817
- Denney, K. D., Bentz, M. C., Peterson, B. M., et al. 2006, *ApJ*, 653, 152
- Di Gesu, L., Costantini, E., Ebrero, J., et al. 2015, *A&A*, 579, A42
- Done, C., Davis, S. W., Jin, C., Blaes, O., & Ward, M. 2012, *MNRAS*, 420, 1848
- Grupe, D., Wills, B. J., Leighly, K. M., & Meusinger, H. 2004, *AJ*, 127, 156
- Guainazzi, M., Perola, G. C., Matt, G., et al. 1999, *A&A*, 346, 407
- Haardt, F. & Maraschi, L. 1991, *ApJ*, 380, L51
- Haardt, F., Maraschi, L., & Ghisellini, G. 1994, *ApJ*, 432, L95
- Haardt, F., Maraschi, L., & Ghisellini, G. 1997, *ApJ*, 476, 620
- Harrison, F. A., Craig, W. W., Christensen, F. E., et al. 2013, *ApJ*, 770, 103
- Jansen, F., Lumb, D., Altieri, B., et al. 2001, *A&A*, 365, L1
- Kaastra, J. S., Kriss, G. A., Cappi, M., et al. 2014, *Science*
- Kaastra, J. S., Petrucci, P.-O., Cappi, M., et al. 2011, *A&A*, 534, A36
- Malizia, A., Molina, M., Bassani, L., et al. 2014, *ApJ*, 782, L25
- Marinucci, A., Matt, G., Kara, E., et al. 2014, *MNRAS*, 440, 2347
- Markowitz, A. G. & Reeves, J. N. 2009, *ApJ*, 705, 496
- Mehdipour, M., Kaastra, J. S., Kriss, G. A., et al. 2015, *A&A*, 575, A22
- Perola, G. C., Matt, G., Cappi, M., et al. 2002, *A&A*, 389, 802
- Petrucci, P.-O., Paltani, S., Malzac, J., et al. 2013, *A&A*, 549, A73
- Piconcelli, E., Jimenez-Bailón, E., Guainazzi, M., et al. 2004, *MNRAS*, 351, 161
- Reynolds, C. S., Brenneman, L. W., Wilms, J., & Kaiser, M. E. 2004, *MNRAS*, 352, 205
- Sobolewska, M. A. & Papadakis, I. E. 2009, *MNRAS*, 399, 1597
- Soldi, S., Beckmann, V., Baumgartner, W. H., et al. 2014, *A&A*, 563, A57
- Strauss, M. A., Huchra, J. P., Davis, M., et al. 1992, *ApJS*, 83, 29
- Ursini, F., Boissay, R., Petrucci, P.-O., et al. 2015, *A&A*, 577, A38
- Walton, D. J., Nardini, E., Fabian, A. C., Gallo, L. C., & Reis, R. C. 2013, *MNRAS*, 428, 2901